lubricants

MDPI

Article

Use of Functionalized Graphene-Based Materials on Grease

Eduardo Tomanik [1,*], Paulo Berto [2], Wania Christinelli [1], Gabriela Papoulias [2], Xavier Raby [1] and Valdirene Peressinotto [1]

[1] Gerdau Graphene, Sao Paulo 05424-050, Brazil; wania.christinelli@gerdaugraphene.com (W.C.); xavier.raby@gerdaugraphene.com (X.R.); valdirene.peressinotto@gerdaugraphene.com (V.P.)
[2] Instituto de Pesquisas Tecnologicas, Sao Paulo 05508-901, Brazil; paulo.berto@ensino.ipt.br (P.B.); papoulias@ipt.br (G.P.)
* Correspondence: eduardo.tomanik@ex.gerdaugraphene.com

Abstract: The growing awareness of reduced friction losses and new demands for electrical powertrains demand improved lubricants. Due to their unique properties, such as high thermal and electrical conductivity, graphene and its derivatives have been investigated for tribological applications, especially as lubricant additives. In this work, we investigated three commercially available graphene variants, one comprising a few layers and the other two comprising nanoplates, after functionalization as additives to lithium soap grease. The grease temperature dropping point increased by approximately 6 °C. Additionally, during the reciprocating friction test, friction increased with the test duration for the baseline grease, whereas it decreased for the ones containing graphene-based additives. On the test end, friction was reduced by 8% compared to the baseline grease. On a four-ball tribometer, the wear scar was reduced from 10 to 18% compared to the baseline grease. In general, no significant difference was seen between the three graphene-based variants. The promising results found with graphene nanoplates, a less expensive material than a few graphene layers, creates opportunities for a cost-competitive additive to commercial greases.

Keywords: graphene; nano-carbon; grease; friction; wear

Citation: Tomanik, E.; Berto, P.; Christinelli, W.; Papoulias, G.; Raby, X.; Peressinotto, V. Use of Functionalized Graphene-Based Materials on Grease. *Lubricants* **2023**, *11*, 452. https://doi.org/10.3390/lubricants11100452

Received: 1 August 2023
Revised: 14 September 2023
Accepted: 4 October 2023
Published: 20 October 2023

1. Introduction

Graphene, a novel 2D material, is being explored for a myriad of applications, from electronic devices to additives for polymers, painting, concrete, etc. [1–3]. Graphene also has great potential as an additive for tribological applications and lubricants [4–16]. Its inherent low friction, high stiffness, and thermal conductivity may bring additional tribological benefits. Despite its strict definition as an "allotrope of carbon consisting of a single layer of atoms arranged in a hexagonal lattice nanostructure", the term "graphene" is also used for some variants presenting up to six atom layers. Graphene nanoplatelets (GNP), oxide and reduced oxide graphene, and even micrographite (graphene nanosheets) have also been generically named and called "graphene" for marketing reasons. Other variants, such as graphene oxide, are also called "graphene" (Figure 1). Different applications require graphene variants to pass through a special preparation process to be "functionalized" or "tailored" for proper dispersion and performance [6]. Surfactants, dispersants, and other substances are usually required to produce desirable properties and ensure graphene's stability as a lubricant additive [6]. Graphene's excellent thermal and electrical conductivity can also reduce operational temperatures in tribological applications of machinery components (rolling bearings, gears, etc.), which increases the shelf life of both the mechanical components [17] and lubricant grease [18]. Based on predictive maintenance data [18], the life of a lubricant grease doubles for each 10 °C of temperature reduction during application. The shelf life of components such as gears and rolling bearings also depends on the operational temperature. The increased thermal conductivity of the lubricant, which is

usually an insulant, also has the potential to avoid electro-static-generated corrosion and discharges, which is especially important for battery electric vehicles [19,20].

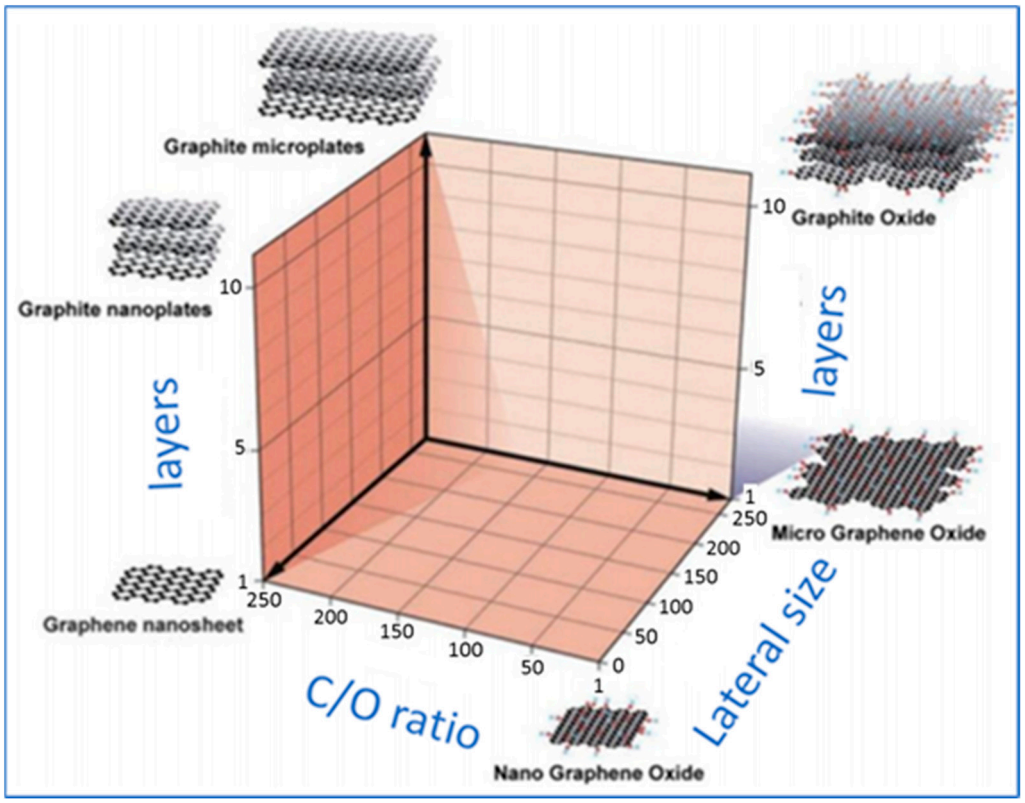

Figure 1. Types of graphene, adapted from Wick et al. [15].

Zero-dimensional (0D) carbon variants such as fullerenes, carbon nano-onions, nanodiamonds, carbon quantum dots, and graphene quantum dots, as well as 1D carbon nanostructures such as carbon nanotubes (CNT) and multi-walled carbon nanotubes (MWCNT), are also being investigated as lubricant additives [6]. For example, Christensen [21,22] observed significant increments in electrical conductivity on lubricant greases using carbon nanotubes (CNT) and carbon nanofibers (CNF).

Graphene's main properties are shown in Table 1.

Table 1. Graphene properties.

Property	Value	Obs.
Elasticity Modulus	1 GPa	5× higher than steel
Rupture Limit	130 GPa	400× higher than steel
Thermal Conductibility	~4000 $W \cdot m^{-1}$	Similar to diamond, 5× higher than copper
Electrical Conductibility	100 $mS \cdot m^{-1}$	40% higher than copper in volume, 6 times in weight
Surface Area	2700 $m^2 \cdot g^{-1}$	2 g has approximately 100 × 50 m

Graphene and other nanoparticles have been extensively investigated for their use in lubricants. The term "nanofluid" is used to describe a fluid containing nanoparticles. Nanofluids' properties depend on the type, size, shape, and concentration of nanoparticles in the fluid, as well as on the stability of the particles in the fluid [5]. Graphene is a unique nanomaterial for lubrication due to its high thermal conductivity and inherent low friction, caused by a weak interaction between individual layers.

In industrial applications, graphene samples present a distribution in terms of size, layers, etc. Even for laboratory-made samples consisting of mostly graphene particles with one to six layers, the relative share of such small particles in area and volume will

be lower than for larger particles. Figure 2 shows the relative share of particles and the respective area and volume for two graphene samples. For the graphene sample with a few layers, in Figure 2a, particles with one to five atom layers represent 77% of the total but only 16.9% of the area and less than 5% of the sample volume. For the graphene oxide (GO) nanosheet sample, in Figure 2b, particles with one to five layers represent 93% of the total but only 53 and 23% of the sample area and volume, respectively. The contributions to the performance of different sub-populations are still unknown and are probably different due to the different properties. For example, friction and wear are probably more influenced by the nanoparticle area and volume, whereas electrical and thermal conductivity are influenced by the number of such nanoparticles.

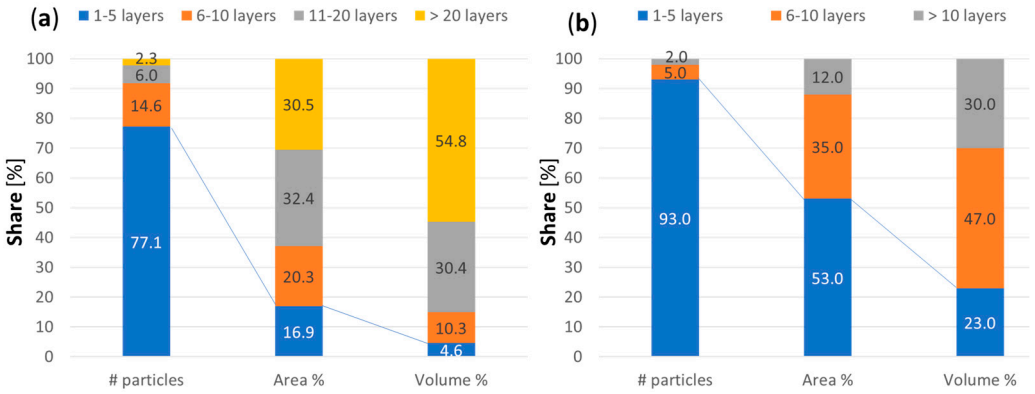

Figure 2. Number of layers, area, and volume. (**a**) Graphene of few layers, data from MGgrafeno; (**b**) GO nanosheets, adapted from [23].

Automotive greases commonly use mineral oil as their fluid components, and these mineral-oil-based greases generally perform satisfactorily in most applications. For more demanding temperatures (low or high), synthetic-oil-based grease provides a better product. Combining a grease thickener with a selected base oil will produce a typical solid-to-semi-fluid grease structure. Lithium soaps are the main types of grease thickener, but other thickeners, such as polyurea, organophilic clay, fumed silica, and fluoropolymers, are also available for specific applications.

Grease lubrication can be divided into three phases/mechanisms [24]: (a) the churning phase, characterized by a fresh-filled grease macroscopic flow whose lubrication regime can be considered fully flooded; (b) bleeding, when the grease releases oil by phase separation via a balance of oil supply and loss mechanisms—this regime can be considered starved elasto-hydro-lubrication (EHL); (c) finally, in extreme cases, no lubricant film exists, causing metal–metal contact, and seizure can occur. The grease must stay in contact with and lubricate moving surfaces without leaking under gravity or centrifugal action or being squeezed out under pressure to properly function. However, such grease consistency may prevent optimal lubrication performance if the grease is pushed out of the bearing and no longer actively participates in the lubrication process. Additives are used to improve the desirable properties and/or suppress undesirable ones. The most common grease additives are oxidation and rust inhibitors. In applications where extreme pressure contacts are present, sulfur-based and other extreme pressure additives are used. The grease thickener can form tribofilms and play some role when contact occurs [25]. Solid particulate additives such as molybdenum disulfide or graphite have become more common, with a present focus on increasing the energy efficiency and time between maintenance and reducing the cost of ownership. Most lubricant additives contain heavy metals such as Zn, Cu, Pb, etc., or involve sulfur atoms [24,26–28], which pose potential environmental threats. In addition to its low environmental impact, graphene's two-dimensional structure and properties make it a potential candidate to replace other materials used as additives in the grease lubricant industry. Studies reported in Liu's review [8] state that the high thermal conductivity of graphene promotes the dissipation of heat generated during sliding motion.

As an additive, graphene offers enhanced thermal stability in addition to lower friction, a lower wear rate, and enhanced load-bearing capacity compared to graphite. As a grease additive, it was observed that graphene platelets (2 to 15 nm) significantly reduced wear on bearings submitted to oscillating tests and reached almost a 50% friction reduction when the test sliding speed was lower than 1×10^{-6} m·s^{-1}.

Fan [29] investigated multilayer graphene (MLG) as a solid additive and also when dispersed in a bentone grease. The addition of graphene caused an increase in the dropping point and resistance to cone penetration. Singh [30] added rGO concentrations of 0.2, 0.4, and 0.6 wt% to commercial lithium grease. Friction was reduced by up to 30 and 20% for rolling and sliding-induced rolling contacts, respectively. Vibration and noise were also reduced. Wang [31,32] investigated graphene and graphite in concentrations from 0.2 to 2 wt% on lithium greases. They observed an increase in dropping point and penetration resistance. Friction and wear reduction were observed in a four-ball tribometer. Fu [33] tested 1–4 wt% and found the best tribological results at 2 wt%. Thermal conductivity increased with concentration, reaching a 56% increase at 4 wt% graphene. Pape and Poll [34] tested multilayer graphene platelets with different thicknesses and observed reductions in wear and friction in oscillating and sliding tests. The authors observed that the graphene nanoplatelets covered asperities on the rubbing surfaces while avoiding solid metallic contacts. Ouyang [35] used 3D hierarchical porous graphene sheets (3D HPGS) on commercial grease and observed reduced friction and wear on a four-ball tester. The graphene entered the rubbing interfaces and formed a protective tribofilm, reducing friction and wear in all three tribological tests. Wang [36] investigated 0.5–2.0 wt% of few-layer graphene (FLG) on polyurea grease. The higher the FLG content, the larger the storage and loss moduli of the polyurea grease in rheological tests. Lower wear and friction in a reciprocating test were achieved at low loads at both mild and high temperatures. During the reciprocating tests, FLGs were initially deposited on the metal surfaces, reducing the roughness. Afterward, the FLGs present in the grease enhanced the stiffness of the formed tribofilm. Finally, the thermal conductivity of graphene mitigated tribofilm deterioration and promoted the formation of protective oxide tribofilms. However, above a critical load, the tribological benefits were much lower.

In the current work, three graphene-based materials produced by different processes were investigated as additives to a simple lithium soap based on mineral oil that was used for automotive applications. Section 3.1 describes the three variants in terms of their structure, number of coupled interlayers, lateral size, etc. Dispersing carbon nanostructures in lubricants is not trivial since the nanoparticles tend to agglomerate and subsequently sediment [37]. Graphene dispersion in lubricants is complicated by their high chemical inertness, with little to no affinity for most base fluids [38]. Dispersants and surfactants have many varieties, and the choice significantly depends on the nanoparticles and base fluids used. The surfactant must disperse well in the base fluid and interact with nanoparticles to be effective and obtain good dispersion. One means of solving this problem is by modifying the graphene surface through functionalization with different functional groups (oxygen-based, nitrogen-based, sulfur-based, halogen-based, etc.), ions, molecules, or particles. For example, Christensen [39], Hu [40], and Wang [41] describe challenges involving graphene functionalization. In the current work, the three graphene powders were functionalized and mixed with other substances to improve the dispersion and performance. They were then transformed into additives that were finally mixed with the baseline lithium-based grease (Figure 3). Sections 3.3–3.6 compare the performance of the grease prototypes to that of the base grease.

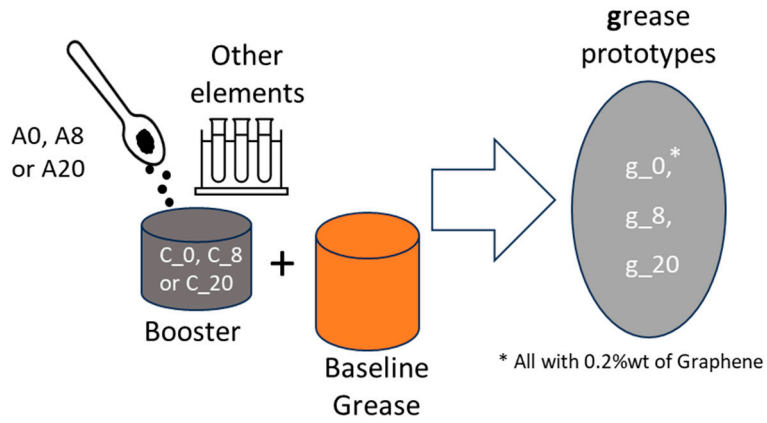

Figure 3. Preparation scheme for the three grease variants used in this work.

2. Materials and Methods

2.1. Graphene Characterization

The graphene samples, after deposition as a powder over a conductive carbon adhesive, were characterized by scanning electron microscopy (SEM) using a Hitachi SU5000 model. Raman spectroscopy (Tokyo, Japan) was used to characterize the crystallinity of the samples using Witec Alpha 300 RA equipment (Ulm, Germany) with a 532 nm laser. To evaluate the influence of crystalline quality on these materials, we measured Raman spectra using protocols to quantify crystalline defects and the number of graphene-coupled interlayers, as described in [41].

2.2. Rheometer

The greases' rheological characterization was performed using an Anton Paar MCR 702 evolution rheometer. A 25 mm plate–plate configuration was used. The temperature was controlled to 25 ± 1 °C. Appendix A discusses other grease prototypes with higher graphene content, which present different rheological behavior.

2.3. Tribological Testers

An Anton Paar TRB^3 and a Falex four-ball extreme pressure test machine (four-ball) were used to investigate friction, wear, and seizure resistance. The sphere was mounted on a stiff cantilever with a frictionless force transducer. The friction force was determined by measuring the deflection of the cantilever. The main equipment and test parameters are described in later sections. Table 2 summarizes the parameters used for the Anton Paar TRB^3 reciprocating test. Each grease sample was tested twice.

Table 2. Parameters used for TRB^3 tests.

Parameter	Description/Amount
Movement/motion/run	Linear reciprocating
Sphere (static part)	Steel 100Cr6 (6 mm)
Sample (counter body)	Steel 52100, commonly used for rolling bearings
Load	5 N
Amplitude (stroke)	6 mm
Maximum linear speed	40 mm·s^{-1}
Frequency	2.12 Hz
Duration	10 min
Temperature	27 ± 1 °C

The 4-ball wear test method is normally used to determine the relative wear-preventing properties of lubricants and greases under test conditions for sliding steel-on-steel applications. The 4-ball tester was used to measure wear and load-carrying capacity (LCC). The

4-ball tester consisted of a rotating upper ball loaded against three stationary lower balls. The load-carrying capacity (LCC), also called the seizure limit, was defined according to ASTM D2596. During the test, the load is increased in steps. At a given load, the lubricant boundary film is lost, welding occurs in the balls, and the test is terminated.

3. Results

3.1. Graphene Characterization

We investigated the graphene morphology of the three variants by scanning electron microscopy (SEM), Raman spectroscopy, thermogravimetric analysis (TGA), and X-ray diffraction (XRD). Figure 4 shows SEM micrographs for the three graphene types, referred to as A0, A8, and A20, respectively. At lower magnification, all the materials present sheet aggregates. As the magnification level increases, it is possible to observe planar/nanosheet structures with heterogeneous size distributions. Table 3 summarizes the main characteristics of the three variants.

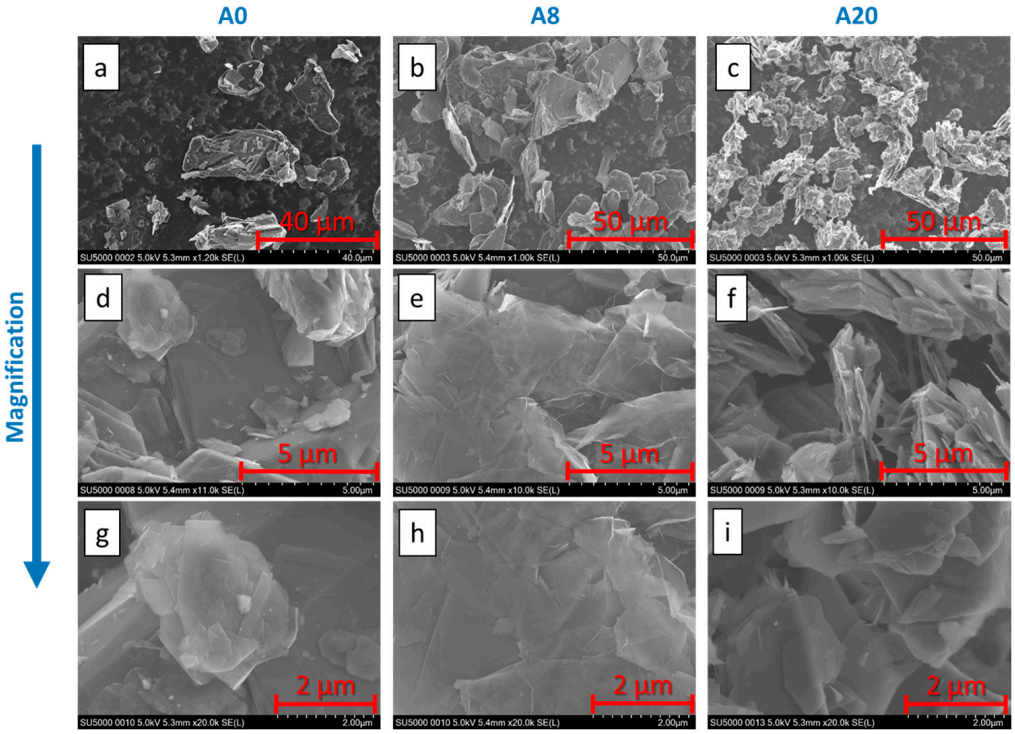

Figure 4. SEM images of the investigated graphene types at 3 different magnification levels. A0: (**a**,**d**,**g**). A8: (**b**,**e**,**h**); A20: (**c**,**f**,**i**).

Table 3. Main characteristics of the graphene-based variants.

	Type	Number of Coupled Interlayers	Primary Sheet Lateral Size	Agglomerate Size [µm]
A0	Graphene nanoplates	≥10	Smaller	~25, spherical
A8	Graphene nanoplates	6 to 10	Medium	~10, sharp edges
A20	Graphene	≤6	Larger	~30

At higher magnification (Figure 4g–i), morphological differences between the three graphene samples appear. A0 sheets are aggregated in a spherical manner, whereas graphene agglomerates from A8 sample sheets exhibit sharp edges. On the other hand, the A20 graphene sheets appear thinner, crimped, and less broken than the two previous samples.

Figure 5 shows the Raman spectra of the three variants. A typical Raman spectrum of graphene has three main bands that describe the crystalline quality of the material and stacking characteristics, such as the number of coupled interlayers. The D band, located at 1350 cm^{-1}, is activated by the disorder generated at 1580 cm^{-1}, caused by stretching the

C-C covalent bonds common in all carbon systems with sp2 hybridization. The 2D band, located at approximately 2700 cm^{-1}, is the overtone of the D band, with two transverse optical phonons.

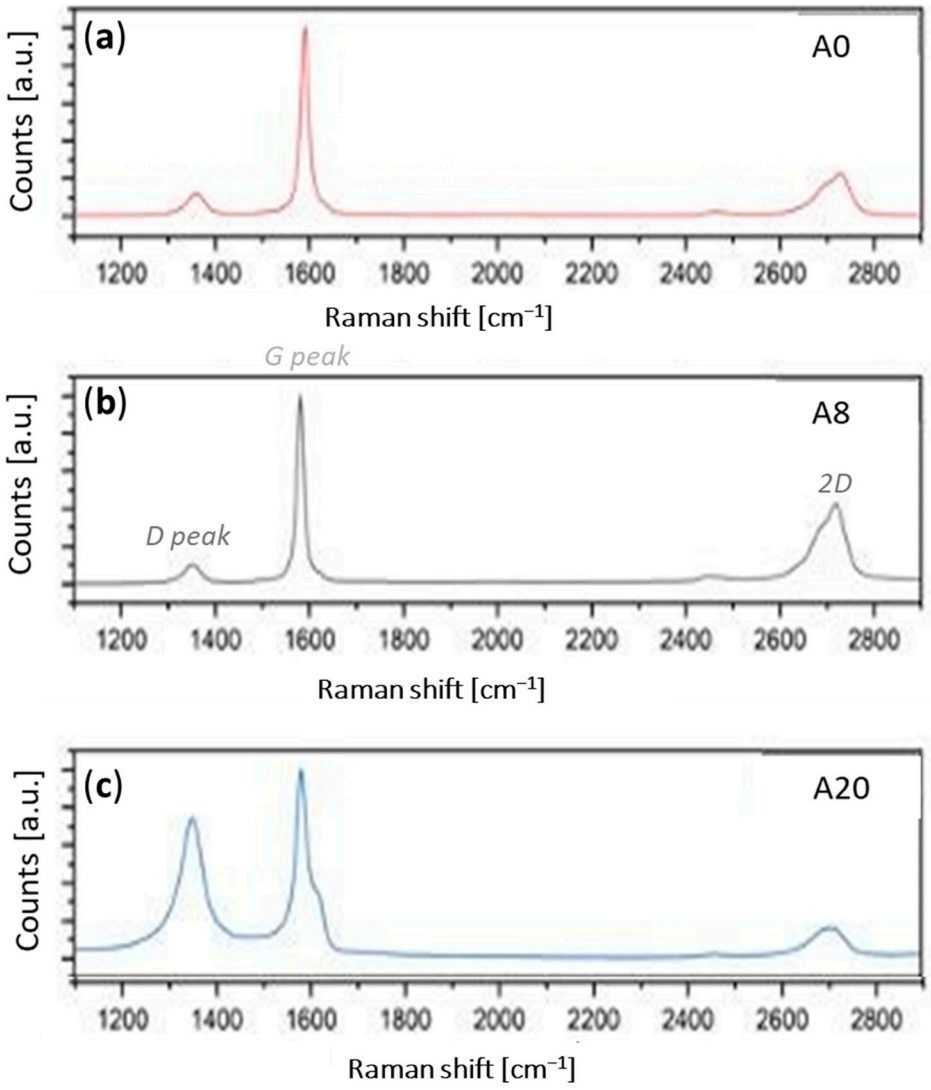

Figure 5. Raman spectra of the three variants: (**a**) A0; (**b**) A8; (**c**) A20. Note: the 2D peak is also referred to as "G" in the literature.

As shown in Figure 5, the A0 and A8 spectra show low intensities and lengths in the D band and low lengths in the G band. The quantification of the characteristics of the materials (Table 3) shows that no significant defects occurred and presents similar behavior for these two samples. The D to G peak intensity ratio (I_D/I_G), the distance between point defects (L_D), and the surface density of point defects (nD) showed the same values at approximately 0.10, 40 nm, and 2 (1010 cm^{-2}), respectively. These results indicated the samples' high crystalline quality. The number of coupled layers <N>2D for A0 and A8 appeared at >10 layers, according to Silva's applied protocol [41]. The 2D band profile for A8 was slightly different from that of A0. However, the applied 2D protocol only inferred the degree of interlayer coupling. The protocol results suggested that A8 should be more easily exfoliated than A0 during the incorporation and functionalization processes in the grease matrix. Less energy would be required to exfoliate graphene-based materials exhibiting a lower interlayer coupling degree. Table 4 summarizes the data obtained from the Raman spectra after using the aforementioned protocol.

Table 4. Data from Raman spectroscopy.

	A0	**A8**	**A20**
I_D/I_G	0.10	0.09	0.73
A_D/A_G	0.25	0.23	1.40
Γ_G [cm^{-1}]	18.5	15.9	28.2
L_a [nm]	79	99	31
L_D [nm]	40	40	9
nD [10^{10} cm^{-2}]	2	2	40
<N>2D	>10	>10	5

When we analyzed the percentage distribution of the number of coupled layers in detail, we could verify that A8 had a greater distribution below 10 layers compared to A0. Figure 6a shows that A0 has 53% of <N>2D above 10 layers, whereas A8 has only 18% (see Figure 6b).

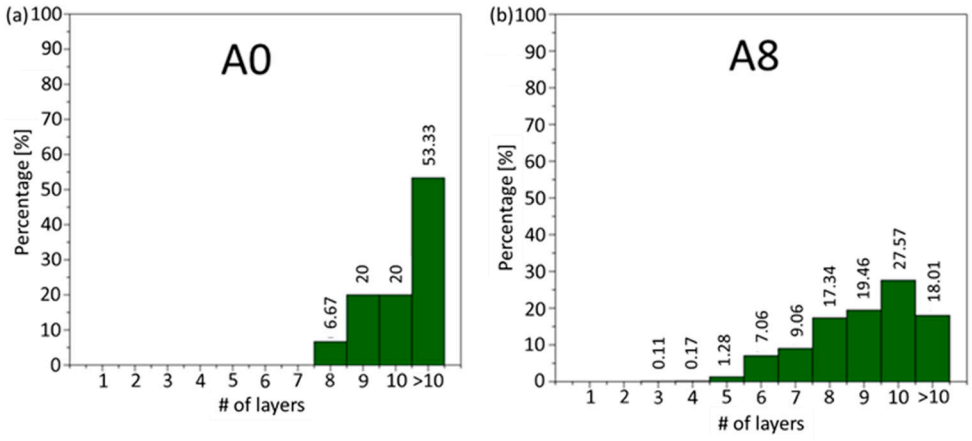

Figure 6. Percentage distribution of the number of coupled layers for (**a**) A0 and (**b**) A8.

The A20 sample presented different Raman spectra. For a better understanding, the A20 data are separated in Figure 7. The A20 spectrum shows an increase in D peak intensity and the D′ appears. The defect types present in graphene can be divided into two groups: (I) defects in the graphene sheet plane (point defects) due to vacancies, folds, creases, stone-wales, and doping by impurities, and (II) edge defects (linear defects) called zigzag and armchair. The intensity of the D and D′ bands in the Raman spectrum shows the level of disorder caused by the defects.

Analyzing the D to G peak intensity ratio (ID/IG), the distance between point defects (LD) and the surface density of point defects (nD), which are 0.73, 9 nm, and 40 (1010 cm^{-2}), respectively, indicate that A20 had a higher level of disorder compared to A0 and A8. A possible explanation for this behavior is that the graphene production method created a higher intercalation level. Additionally, a lower number of decoupled layers was observed for A20 compared to the others (see Figure 8b), suggesting a higher tendency for exfoliation during the incorporation and functionalization process into the grease matrix.

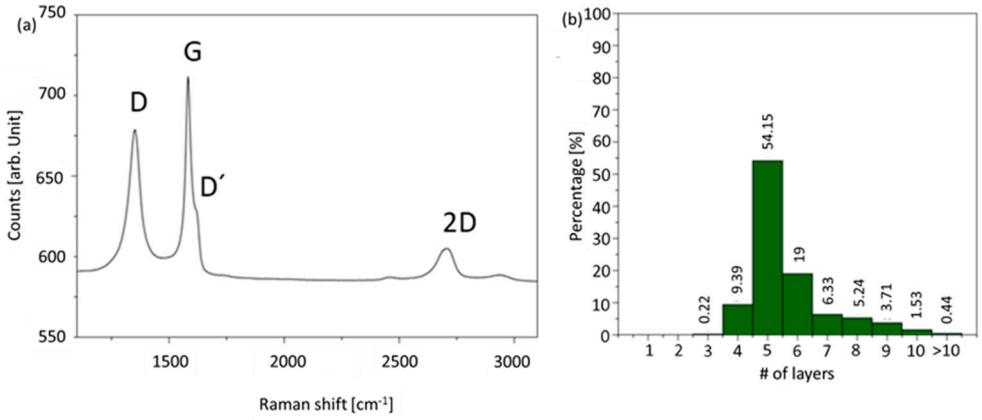

Figure 7. A20 variant. (**a**) Raman spectra; (**b**) percentage distribution of the number of coupled layers.

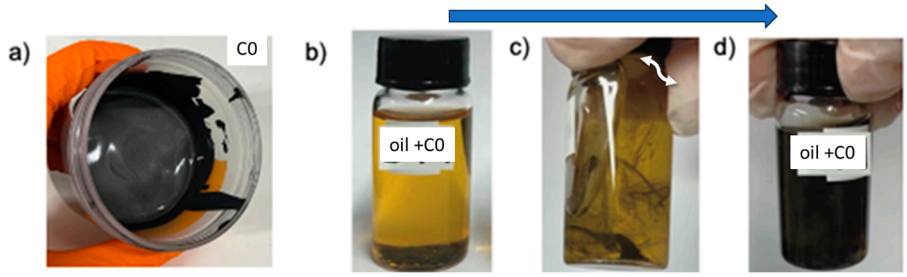

Figure 8. (**a**) Booster with 30% of graphene; (**b**–**d**) manual agitation to illustrate the good dispersion. The final mixture contains 0.2 wt% of graphene for a 0W-20 oil.

3.2. Booster for Grease and Oil Additive

To obtain a good mixture of lubricants, the graphene powders were functionalized with long-chain organic molecules with polar ends before being added to the base grease. Each of the three graphene variants was high-shear-mixed in a concentrated form with approximately 30 wt% graphene for 30 min. To promote the organic molecule and graphene interaction, molecules with oxygenated and nitrogenated groups were used. The substances and methods used for graphene functionalization were proprietary and cannot be detailed here.

The previously described boosters were also investigated as additives to engine and industrial lubricant oils. Oil graphene additives for oils require more physical stability due to the lower oil viscosity. Therefore, the stability of graphene in the oil is easier to evaluate than in lubricant greases. Figures 8 and 9 illustrate the boosters' dispersion and stability in fully formulated engine oil with a viscosity specification of 0W-20.

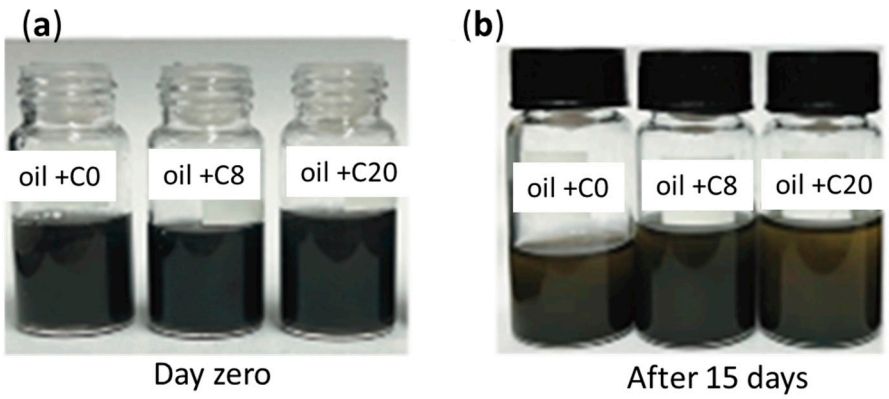

Figure 9. Boosters mixed with SAE 0W-20 engine oil. (**a**) Shortly after mixing. (**b**) After 15 days.

3.3. Grease Sample Preparation

Three boosters, C0, C8, and C20, with high concentrations of the previously mentioned functionalized graphene variants, were mixed with a lithium soap grease with the baseline oil at a viscosity of 150 cSt at 40 °C. To ease mixing, both the boosters and baseline grease were heated to 70 °C in a furnace to reduce the grease consistency. The graphene-based boosters were mixed with the baseline grease using a planetary blender in controlled and scalable lab sample production. See Figure 10. Three consecutive blending sequences of two minutes each were used to achieve a homogeneous mixture. A manual spreader was used before and after each blending sequence, with special attention to separating the mixture from the vessel wall. No equipment was used to improve grease homogenization (e.g., Gaulin Homogenizer or Charlotte Colloid Mill) because it would shear the graphene sheets used in this study.

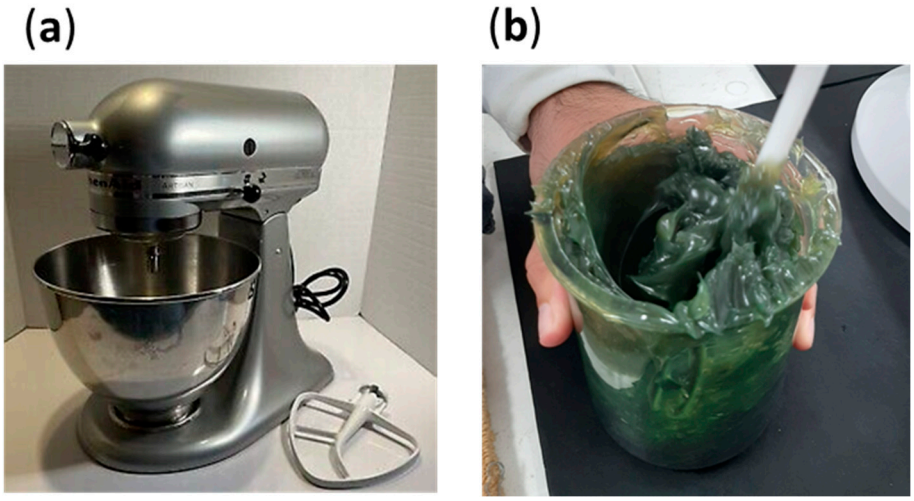

Figure 10. (**a**) Planetary blender and (**b**) manual spreader used between sequences to separate the mixture from the vessel wall.

Approximately 500 g of lubricant grease was produced with each graphene variant, all with a final concentration of 0.2 wt% of the GNP additive. To differentiate the concentrated GNP samples from the resultant greases, the grease samples were denominated as g_0, g_8, and g_20, with respect to variants A0, A8, and A20 (Figure 4). As expected, the grease acquired a blackish color, as seen in Figure 11.

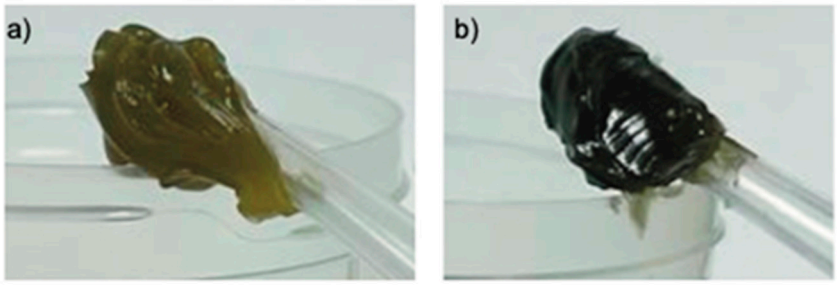

Figure 11. Visual aspect of the grease. (**a**) Before combination with graphene booster; (**b**) after combination with the graphene booster.

3.4. Grease Consistency (Cone Penetration)

The lubricant grease samples, after homogenization, were tested with a Seta Universal Penetrometer. Penetration tests were performed on the petroleum lubricant greases to determine their consistency and shear stability. See Figure 12. A standard cone was released from a penetrometer and allowed to drop freely into the sample for 5 s at a constant temperature. The cone's depth of penetration into the sample was measured

in tenths of a millimeter with a penetrometer. The grease samples were tested following procedures according to ASTM D1403 using half-scale penetration cone equipment. The samples were then "worked" using a Seta High-Temperature Roll Stability Tester to provide an indication of the shear stability by testing the change in worked penetration. The test was conducted according to the test method ASTM D1831. No significant influence on grease consistency was observed (see Table 5).

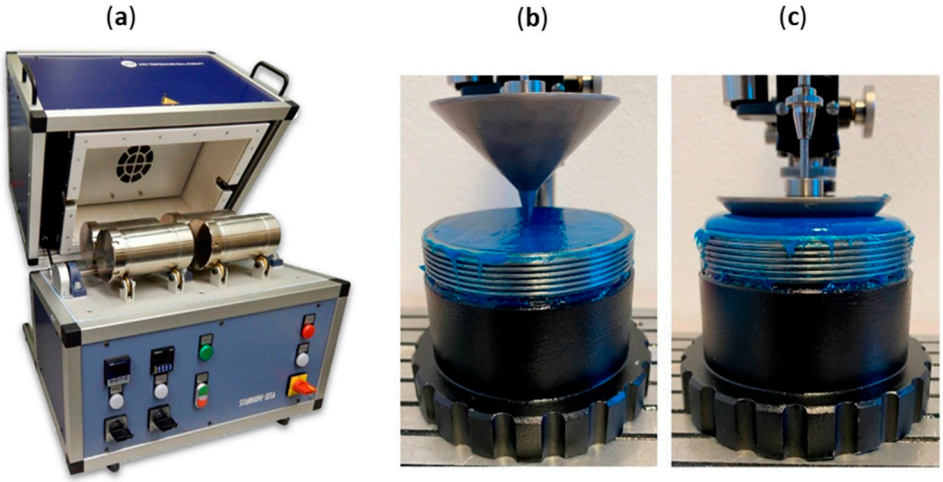

Figure 12. (**a**) Roll stability test with Stanhope Seta. Grease penetration test. (**b**) Before and (**c**) after cone penetration [42].

Table 5. Converted penetration (consistency) 1/10 mm 25 °C.

Sample	As New	After Roll
Baseline	241	259
g_0	241	263
g_8	243	251
g_20	241	265

The roll stability test measured the mechanical stability by rotating a grease sample in a cylinder containing a roller. The cone penetration tests were run before and after rolling, and the results were compared. We observed that the variants did not influence the mechanical stability compared to the base grease.

3.5. Grease Dropping Point

The grease dropping point is the temperature at which the first drop of the fluid (commonly the base oil) separates totally from the grease composition. It indicates the grease's heat resistance and depends on the thickener type used and its cohesiveness in the oil and thickener structure. The dropping point temperature indicates the limit at which the grease retains its structure, although not necessarily the limit for grease usage. For greases where graphene samples were added, slightly higher temperatures were observed at the dropping point (see Figure 13).

Energy conversion dynamically occurs at the atomic level in solid materials through uncontrolled electron diffusion and lattice vibrations. See Figure 14. When graphene is added to a base lubricant, the fluid's thermal conductivity and heat transfer efficiency are often improved. Brownian motion, radiative heat transport, the liquid oil layer around the nanoparticles, and the clustering of nanoparticles have the greatest effects on the thermal conductivity in the lubricant with graphene or other nanoparticles. The Brownian motion of nanoparticles in oil mainly regulates the thermal conductivity of lubricants. The Brownian motion of nanoparticles improves thermal conductivity in several ways,

including nanoparticle collisions that result in heat transfer by solid–solid conduction and heat transfer by convection.

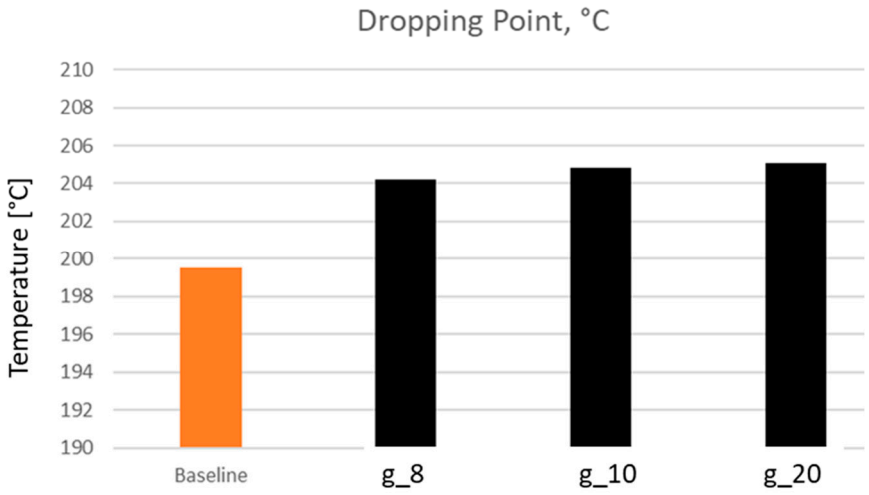

Figure 13. Dropping points of the tested greases.

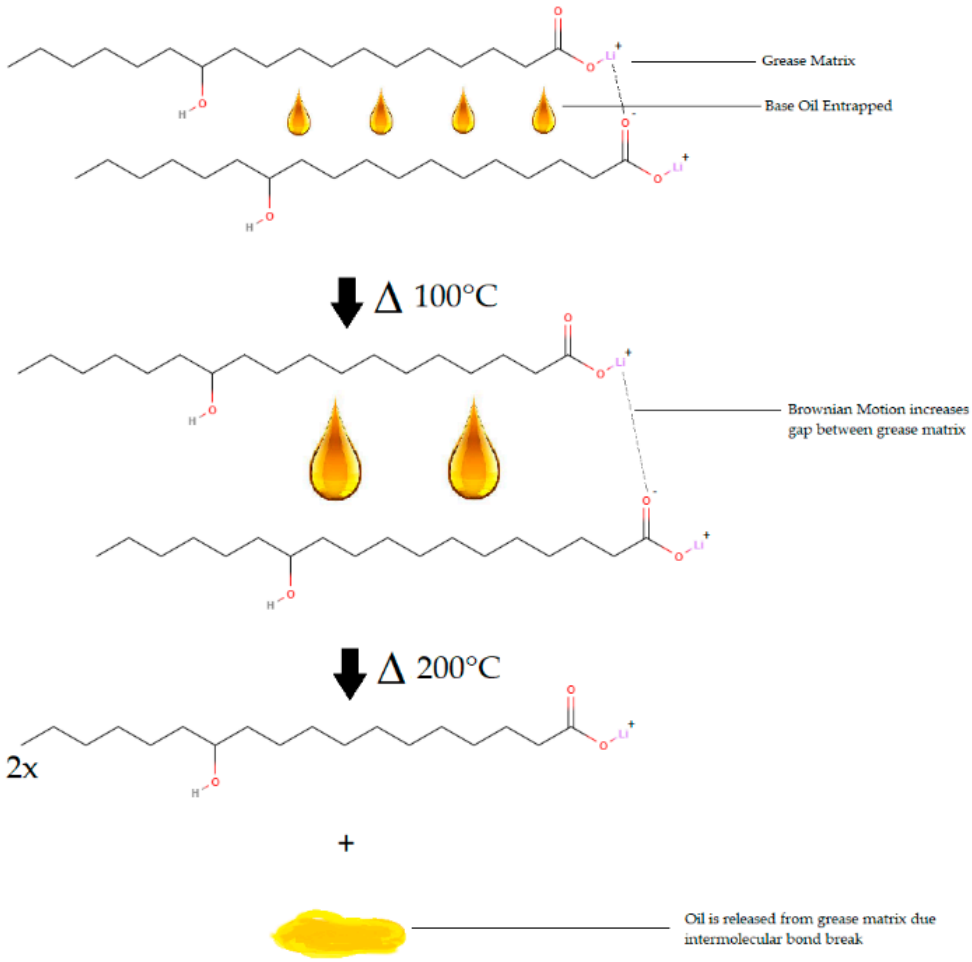

Figure 14. Dropping point at the atomic level of lithium greases.

Compared to other carbon-based materials, graphene has higher thermal conductivity, and, when properly inserted into the grease matrix, it dissipates the heat and strengthens intermolecular bonds, improving the dropping point. We observed that all graphene variants improved the dropping point, with a small difference between the variant g_8 and

the g_0 and g_20 variants. The slightly worse performance might be related to steric effects between the grease matrix and multilayer presented in the g_8 variant.

3.6. Grease Rheology

The variants presented similar behavior regarding grease rheology, except for shear thinning at shear rates >50 s^{-1}, especially for the g_8 and g_20 variants (Figure 15). Different behaviors may occur at higher graphene concentrations (see discussion in Appendix A).

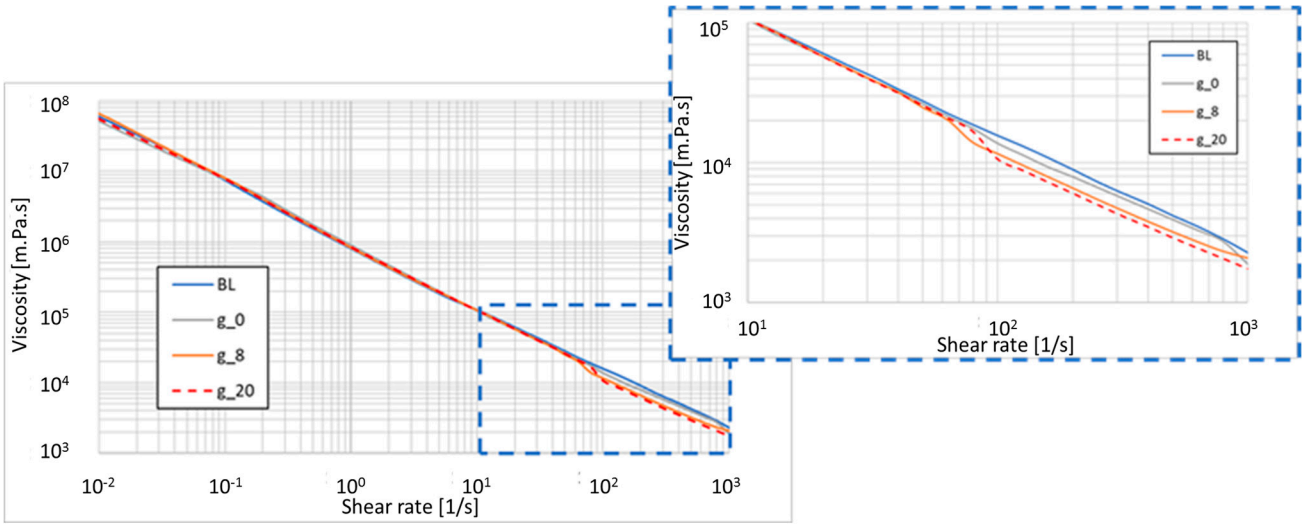

Figure 15. Grease samples' rheology at different shear rates.

3.7. Pin-on-Disk Tribometer TRB³ Test

Under this reciprocating test, the prototype greases presented slightly lower friction, especially with test time evolution. When the test started, the baseline and prototypes presented initially higher friction between 0.13 and 0.14. After a period of stabilization, probably due to grease accommodation and the release of the lubricant oil in the contact region, the baseline friction increased for the baseline grease, while the graphene-based variants exhibited a friction reduction, as seen in Figure 16. After 600 s, greases with graphene presented around 5% lower friction than the baseline.

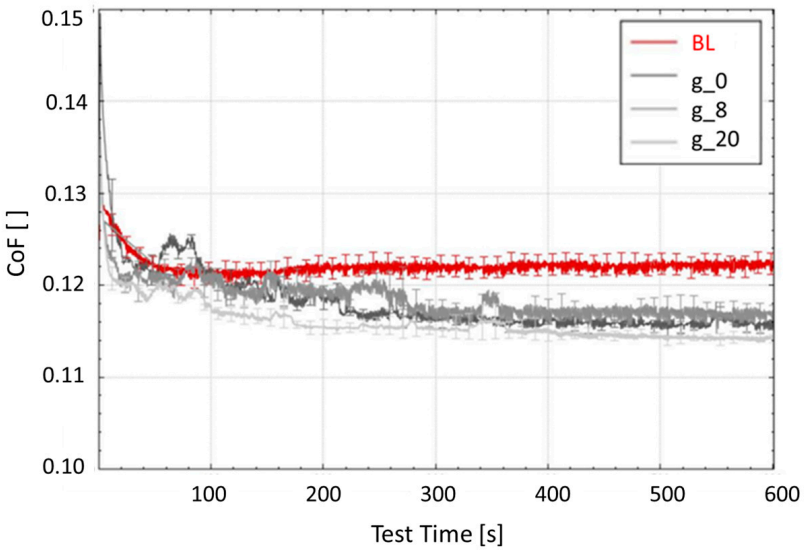

Figure 16. Friction along the reciprocating tribological test.

3.8. Four-Ball Wear Test

The samples were also submitted to a four-ball wear tester. As shown in Figure 17, the graphene additives reduced wear compared to the baseline grease, and the prototypes all performed similarly.

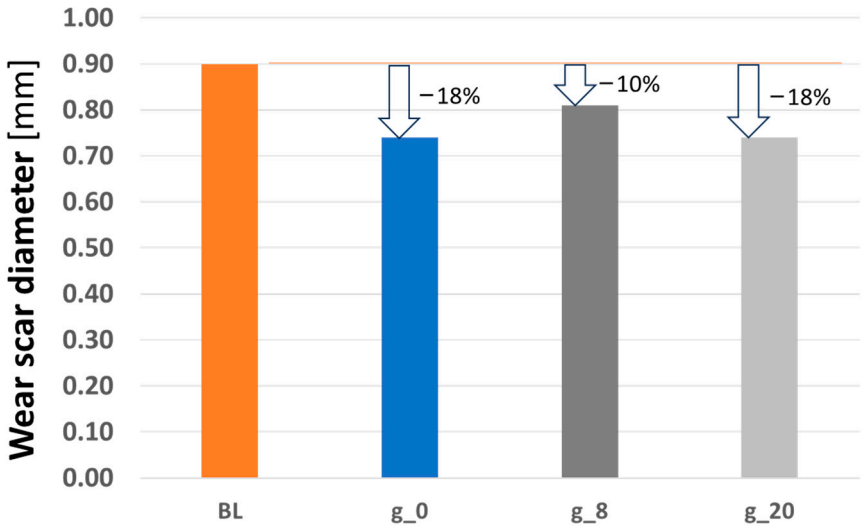

Figure 17. Wear scar diameter on 4-ball wear test.

3.9. Four-Ball EP Test

The greases were also tested for seizure in a four-ball EP tester. This test is used to determine the extreme pressure (EP) characteristics of lubricating greases in sliding steel-on-steel applications. Measurements of rotating speeds, temperatures, and duration were recorded as specified by the standard method ASTM D2596. The test was stopped when noise indicated that a seizure had occurred. Since the baseline grease had no EP additive, the seizure limit was relatively low. Due to this, all graphene-added grease samples were tested initially with a small load of 126 kgf. Instead of the typical welded pyramid-like ball, the tested balls became loose after the tests (Figure 18).

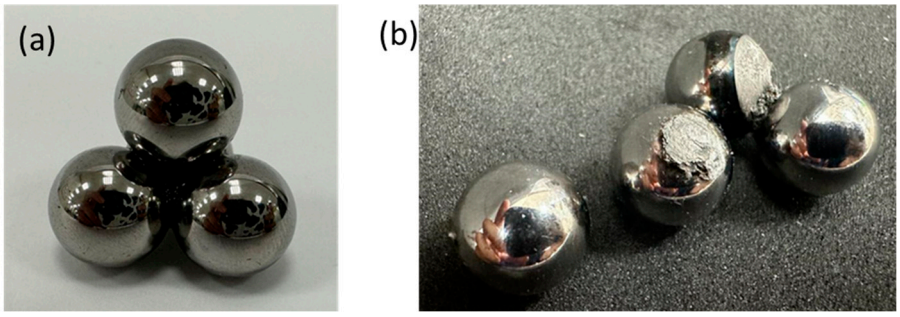

Figure 18. (**a**) Pyramid-like welded balls after typical 4-ball seizure test; (**b**) balls loose after the test.

4. Discussion

The higher temperatures found for samples with graphene additives on the dropping point test are beneficial for most applications, which could be due to improved thermal conductivity and/or the graphene booster's effect on grease cohesiveness at elevated temperatures. Further studies are needed to investigate these effects.

We analyzed the wear track on balls tested with graphene using Raman spectra and found evidence of boundary tribolayer formation. Similar effects were observed in tribological tests on engine oils with the same boosters used for the greases, which will be the subject of a future publication. We posit that the graphene layer synergy and the tribochemical layer enhanced the lubricating performance. Figure 19 shows balls tested

with graphene boosters. The test was stopped after welding (torque increase) indications. However, the balls were not fully welded after disassembly. Wear track and material transfer could be seen on the tested balls, but they were not solidly welded. After the baseline and g_8 tests, four spheres were damaged but not welded, g_0 tests presented two semi-welded spheres, and g_20 tests presented three.

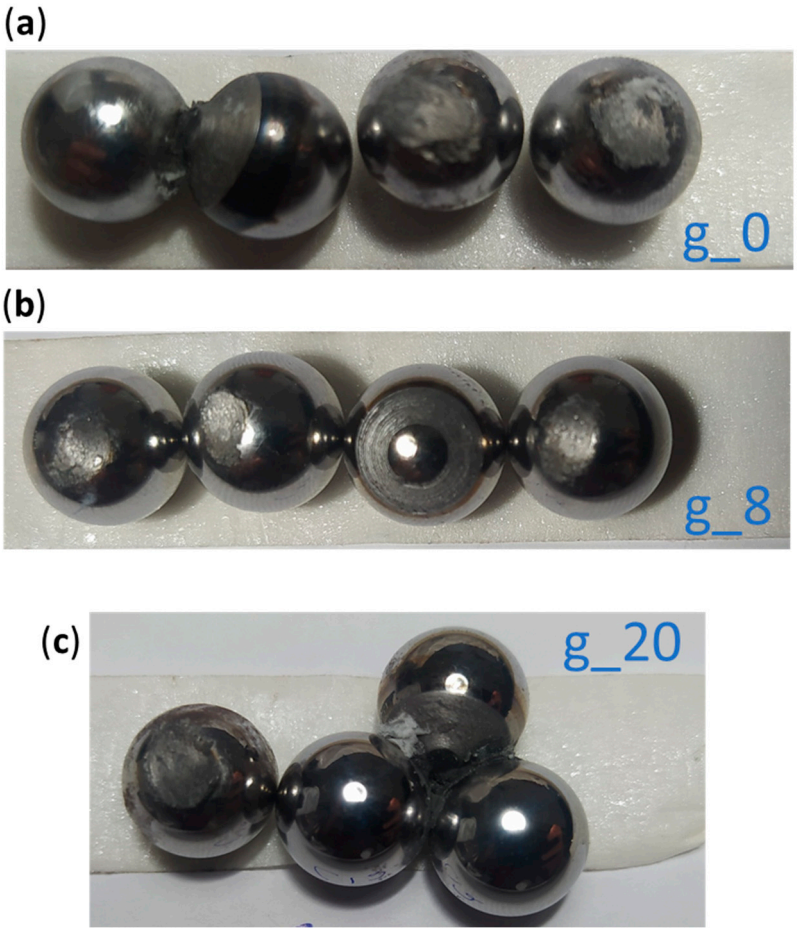

Figure 19. Balls after 4-ball seizure test with graphene additives. (**a**) Tested with g_0; (**b**) tested with g_8; (**c**) tested with g_20.

5. Conclusions

The modified greases presented improved thermal and tribological properties. The grease temperature dropping point increased by approximately 6 °C and friction was reduced by 10% compared to baseline grease. During the reciprocating friction test, friction increased with the test duration for the baseline grease, whereas it decreased for graphene-based additives. Nonetheless, the three graphene-based materials exhibited a meaningful disparity in their physical properties and no significant difference was observed. Two main assumptions were considered for this observation.

- The tribological properties measured in this study may not have been sensitive to the amplitude of variation measured in the three graphene-based materials' characteristics presented, such as the number of coupled layers, crystallinity, and morphology of primary sheets and aggregates.
- Functionalization and incorporation processes might have "smoothed" the disparities between the three graphene-based materials in their dispersed form in the grease matrix compared to their initial physical properties as powders. The development of graphene characterization techniques in a grease environment would be required to validate these assumptions.

Nonetheless, these graphene-based materials are less expensive than few-layer graphene, offer promising results, and present opportunities for cost-competitive additives in commercial greases that will be explored in future studies.

Author Contributions: Conceptualization, E.T., W.C. and P.B.; methodology, all co-authors; investigation, W.C., P.B., X.R. and G.P.; writing—original draft preparation, E.T., W.C., P.B., X.R. and G.P.; writing—review and editing, E.T., G.P. and V.P.; supervision, V.P.; project administration, V.P. All authors have read and agreed to the published version of the manuscript.

Funding: The work was partially funded by Fundação de Desenvolvimento da Pesquisa—Fundep Rota 2030—Linha V.

Acknowledgments: The authors would like to acknowledge Anton Paar, Brazil, where some characterizations and tests were performed, and whose team helped us to determine which techniques to use to analyze the results.

Conflicts of Interest: The authors declare no conflict of interest. The funders had no role in the design of the study; in the collection, analyses, or interpretation of data; in the writing of the manuscript, or in the decision to publish the results.

Appendix A. Rheology—Shear Thinning with Some Graphene Variants

As previously mentioned, additive effects strongly depend on the graphene concentration and applied functionalization. Graphene has also shown benefits for hydrodynamic lubrication regimes, which hardly can be explained only by typical friction modifier surface effects. Moreover, 2D additives are known to change the lubricant rheology. Two recent works (Giudice [43], Hamze [44]) reviewed dozens of references about the rheology of graphene-based materials. However, most of the works focused on aqueous dispersions or polymers, and few discussed tribological effects. Wang and Gao [45] used few-layer graphene (FLG) as a nano-additive to lithium complex grease and investigated the FLG's influence on viscoelasticity and friction. The FLG changed continuously between two agglomeration states and its ordering affected the friction behavior during the tests. Graphene sheets assumed different ordering and agglomeration under the shearing stress caused by the test.

In a previous experiment, a booster C0 was mixed to reach 0.10, 0.15, and 1.00 wt% A0 concentrations (plus the functionalization elements). Different from the mixing described in this study, we used a high-energy method to mix the booster with the baseline grease. The grease rheology was significantly affected by the 0.5 and 1.0 wt% concentrations (Figure A1). The viscosity increased at low shear rates and was reduced at shear rates higher than approximately $2 \times 10\ s^{-1}$.

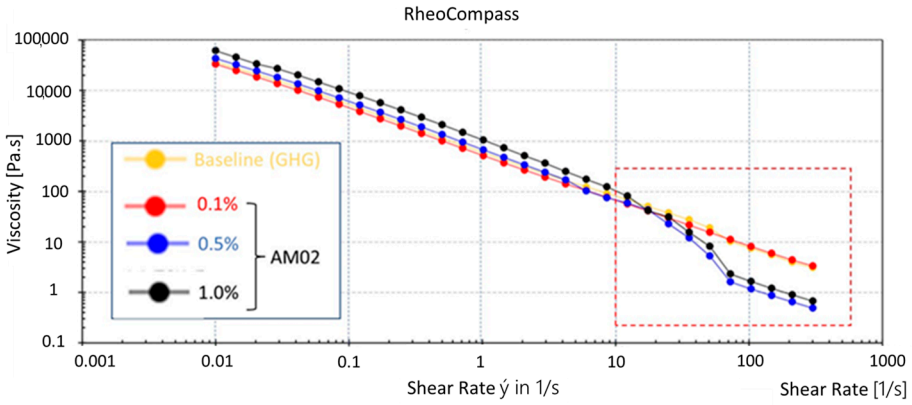

Figure A1. Grease rheology using C0 mixed with grease using high-energy methods.

We postulate that greases can be considered long-chain molecules where the viscosity is dominated by physical entanglements between molecules. The typical pseudoplastic behavior illustrates this concept (baseline Figure A1). Graphene sheets are randomly oriented

at low shear rates, causing an increase in viscosity from the perpendicular orientation of some of the graphene sheets to fluid flow. Graphene sheets are aligned with fluid flow at higher shear rates and, consequently, cease contributing to the increased viscosity. The additional drop observed in Figure A1 for shear rates higher than $2 \times 10\ s^{-1}$ in variants with 0.5 and 1.0% may be due to the graphene sheets increasing the distance between long-chain molecules and making physical entanglement less likely (Figure A2).

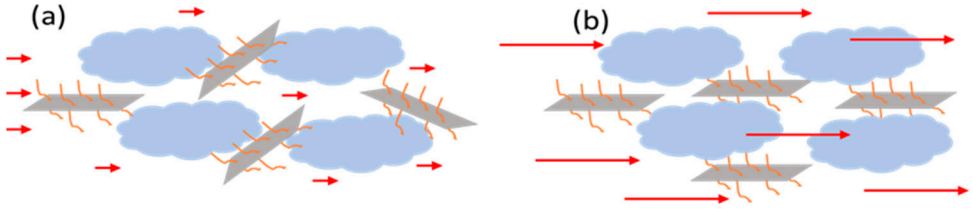

Figure A2. Scheme of 2D materials' potential effect on rheology. (**a**) At low shear rate, (**b**) at higher shear rates.

References

1. Georgakilas, V.; Perman, J.A.; Tucek, J.; Zboril, R. Broad Family of Carbon Nanoallotropes: Classification, Chemistry, and Applications of Fullerenes, Carbon Dots, Nanotubes, Graphene, Nanodiamonds, and Combined Superstructures. *Chem. Rev.* **2015**, *115*, 4744–4822. [CrossRef] [PubMed]
2. Ren, W.; Cheng, H.M. The global growth of graphene. *Nat. Nanotechnol.* **2014**, *9*, 726–730. [CrossRef] [PubMed]
3. Zhu, Y.; Ji, H.; Cheng, H.M.; Ruoff, R.S. Mass production and industrial applications of graphene materials. *Natl. Sci. Rev.* **2018**, *5*, 90–101. [CrossRef]
4. Berman, D.; Erdemir, A.; Sumant, A. Graphene: A new emerging lubricant. *Mater. Today* **2014**, *17*, 31–42. [CrossRef]
5. Penkov, O.V. *Tribology of Graphene Simulation Methods, Preparation Methods, and Their Applications*; Elsevier: Amsterdam, The Netherlands, 2020. [CrossRef]
6. Nyholm, N.; Espallargas, N. Functionalized carbon nanostructures as lubricant additives—A review. *Carbon* **2023**, *201*, 1200–1228. [CrossRef]
7. Liu, Y.; Ge, X.; Li, J. Graphene lubrication. *Appl. Mater. Today* **2020**, *20*, 100662. [CrossRef]
8. Liu, L.; Zhou, M.; Jin, L.; Li, L.; Mo, Y.; Su, G.; Li, X.; Zhu, H.; Tian, Y. Recent advances in friction and lubrication of graphene and other 2D materials: Mechanisms and applications. *Friction* **2019**, *7*, 199–216. [CrossRef]
9. Bao, T.; Wang, Z.; Zhao, Y.; Wang, Y.; Yi, X. Long-term stably dispersed functionalized graphene oxide as an oil additive. *RSC Adv.* **2019**, *9*, 39230–39241. [CrossRef]
10. Gao, Q.; Liu, S.; Hou, K.; Li, Z.; Wang, J. Graphene-Based Nanomaterials as Lubricant Additives: A Review. *Lubricants* **2022**, *10*, 273. [CrossRef]
11. Chouhan, A. Chemically functionalized graphene for lubricant applications: Microscopic and spectroscopic studies of contact interfaces to probe the role of graphene for enhanced tribo-performance. *J. Colloid Interface Sci.* **2018**, *513*, 666–676. [CrossRef]
12. Gulzar, M.; Masjuki, H.H.; Kalam, M.A.; Varman, M.; Zulkifli, N.W.M.; Mufti, R.A.; Zahid, R. Tribological performance of nanoparticles as lubricating oil additives. *J. Nanopart. Res.* **2016**, *18*, 223. [CrossRef]
13. Lau, G.A.; Neves, G.O.; Salvaro, D.B.; Binder, C.; Klein, A.N.; de Mello, J.D.B. Stability and Tribological Performance of Nanostructured 2D Turbostratic Graphite and Functionalised Graphene as Low-Viscosity Oil Additives. *Lubricants* **2023**, *11*, 155. [CrossRef]
14. Liu, Y.; Yu, S.; Shi, Q.; Ge, X.; Wang, W. Graphene-Family Lubricant Additives: Recent Developments and Future Perspectives. *Lubricants* **2022**, *10*, 215. [CrossRef]
15. Wick, P.; Louw-Gaume, A.; Kucki, M.; Krug, H.; Kostarelos, K.; Fadeel, B.; Dawson, K.; Salvati, A.; Vásquez, E.; Ballerini, L. Classification Framework for Graphene-Based Materials. *Angew. Chem. Int. Ed.* **2014**, *53*, 7714–7718. [CrossRef] [PubMed]
16. Rahman, M.; Islam, M.; Roy, R.; Younis, H.; AlNahyan, M.; Younes, H. Carbon Nanomaterial-Based Lubricants: Review of Recent Developments. *Lubricants* **2022**, *10*, 281. [CrossRef]
17. Morales-Espejel, G.E.; Gabelli, A. A model for rolling bearing life with surface and subsurface survival: Surface thermal effects. *Wear* **2020**, *460–461*, 203446. [CrossRef]
18. Lugt, P.M. On the use of the Arrhenius equation to describe the impact of temperature on grease life. *Tribol. Int.* **2023**, *179*, 108142. [CrossRef]
19. Mustafa, W.; Dassenoy, F.; Sarno, M.; Senatore, A. Senatore A review on potentials and challenges of nanolubricants as promising lubricants for electric vehicles. *Lubr. Sci.* **2022**, *34*, 1–29. [CrossRef]
20. Canter, N. *Tribology and Lubrication for E-Mobility: Findings from the Inaugural STLE Conference on Electric Vehicles*; Society of Tribologists and Lubrication Engineers: Park Ridge, IL, USA, 2022.
21. Christensen, G.; Yang, J.; Lou, D.; Hong, G.; Hong, H.; Tolle, C.; Widener, C.; Bailey, C.; Rob Hrabe, R.; Hammad Younes, H. Carbon nanotubes grease with high electrical conductivity. *Synth. Met.* **2020**, *268*, 116496. [CrossRef]

22. Christensen, G.; Younes, H.; Hong, G.; Lou, D.; Hong, H.; Widener, C.; Bailey, G.; Hrab, R. Hydrogen bonding enhanced thermally conductive carbon nano grease. *Synth. Met.* **2020**, *259*, 116213. [CrossRef]
23. Cremonezzi, J.; Ribeiro, H.; Andrade, R.; Fechine, G. Characterization strategy for graphene oxide and molybdenum disulfide: Proceedings based on the ISO/TS 21356-1:2021 standard. *FlatChem* **2022**, *36*, 100448. [CrossRef]
24. Lugt, P.M. Modern advancements in lubricating grease technology. *Tribol. Int.* **2016**, *97*, 467–477. [CrossRef]
25. Cann, P.M.E. Understanding grease lubrication. *Tribol. Ser.* **1996**, *31*, 573–581. [CrossRef]
26. Fish, G. The development of energy efficient greases. *ELGI EuroGrease* **2015**, *2*, 6–17.
27. Spikes, H. Friction Modifier Additives. *Tribol. Lett.* **2015**, *60*, 5. [CrossRef]
28. Tang, Z.; Li, S. A review of recent developments of friction modifiers for liquid lubricants (2007–present). *Curr. Opin. Solid State Mater. Sci.* **2014**, *18*, 119–139. [CrossRef]
29. Fan, X. Multilayer Graphene as a Lubricating Additive in Bentone Grease. *Tribol. Lett.* **2014**, *55*, 455–464. [CrossRef]
30. Singh, J.; Anand, G.; Kumar, D.; Tandon, N. Graphene based composite grease for elastohydrodynamic lubricated point contact. *IOP Conf. Ser. Mater. Sci. Eng.* **2016**, *149*, 012195. [CrossRef]
31. Jing, W. Tribological Characteristics of Graphene as Lithium Grease Additive. *China Pet. Process. Petrochem. Technol. Lubr. Res.* **2017**, *19*, 46–54.
32. Wang, J.; Guo, X.; He, Y.; Jiang, M.; Gu, K. Tribological characteristics of graphene as grease additive under different contact forms. *Tribol. Int.* **2018**, *127*, 457–469. [CrossRef]
33. Fu, H.; Yan, G.; Li, M.; Wang, H.; Chen, Y.; Yan, C.; Lin, C.T.; Jiang, N.; Yu, J. Graphene as a nanofiller for enhancing the tribological properties and thermal conductivity of base grease. *RSC Adv.* **2019**, *9*, 42481–42488. [CrossRef] [PubMed]
34. Pape, F.; Poll, G. Investigations on Graphene Platelets as Dry Lubricant and as Grease Additive for Sliding Contacts and Rolling Bearing Application. *Lubricants* **2020**, *8*, 3. [CrossRef]
35. Ouyang, T. Friction-reducing and anti-wear properties of 3D hierarchical porous graphene/multi-walled carbon nanotube in castor oil under severe condition: Experimental investigation and mechanism study. *Wear* **2022**, *498–499*, 204302. [CrossRef]
36. Wang, Y.; Gao, X.; Zhang, P.; Fan, Y. Mechanism of Influence of Graphene on Rheological and Tribological Properties of Polyurea Greases Considering Temperature and Load Effects. *Tribol. Lett.* **2023**, *71*, 56. [CrossRef]
37. Ali, I.; Kucherova, A.; Memetov, N.; Pasko, T.; Ovchinnikov, K.; Pershin, V.; Kuznetsov, D.; Galunin, E.; Grachev, V.; Tkachev, A. Advances in carbon nanomaterials as lubricants modifiers. *J. Mol. Liq.* **2019**, *279*, 251–266. [CrossRef]
38. Martin, J.M.; Ohmae, N. *Colloidal Lubrication: General Principles*; Wiley: Hoboken, NJ, USA, 2008.
39. Christensen, G.; Younes, H.; Hong, H.; Peterson, G.P. Alignment of Carbon Nanotubes Comprising Magnetically Sensitive Metal Oxides by Nonionic Chemical Surfactants. *J. Nanofluids* **2013**, *2*, 25–28. [CrossRef]
40. Wang, M.; Zhou, M.; Li, X.; Luo, C.; You, S.; Chen, X.; Mo, Y.; Zhu, H. Research progress of surface-modified graphene-based materials for tribological applications. *Mater. Res. Express* **2021**, *8*, 042002. [CrossRef]
41. Silva, D.L.; Campos, J.L.E.; Fernandes, T.F.; Rocha, J.N.; Machado, L.R.; Soares, E.M.; Miquita, D.R.; Miranda, H.; Rabelo, C.; Neto, O.P.V.; et al. Raman spectroscopy analysis of number of layers in mass-produced graphene flakes. *Carbon* **2020**, *161*, 181–189. [CrossRef]
42. Gurt, A.; Khonsari, M.M. Testing Grease Consistency. *Lubricants* **2021**, *9*, 14. [CrossRef]
43. Giudice, F.; Shen, A. Shear rheology of graphene oxide dispersions. *Curr. Opin. Chem. Eng.* **2017**, *16*, 23–30. [CrossRef]
44. Hamze, S.; Cabaleiro, D.; Estellé, P. Graphene-based nanofluids: A comprehensive review about rheological behavior and dynamic viscosity. *J. Mol. Liq.* **2021**, *325*, 115207. [CrossRef]
45. Wang, Y.; Gao, X.; Lin, J.; Zhang, P. Rheological and Frictional Properties of Lithium Complex Grease with Graphene Additives. *Lubricants* **2022**, *10*, 57. [CrossRef]